



# UNIVERSITÀ DI PARMA

## ARCHIVIO DELLA RICERCA

University of Parma Research Repository

Non-contact direct measurement of the magnetocaloric effect in thin samples

This is the peer reviewed version of the following article:

*Original*

Non-contact direct measurement of the magnetocaloric effect in thin samples / Cugini, Francesco; Porcari, Giacomo; Solzi, Massimo. - In: REVIEW OF SCIENTIFIC INSTRUMENTS. - ISSN 0034-6748. - 85(2014), pp. 074902-1-074902-5. [10.1063/1.4890394]

*Availability:*

This version is available at: 11381/2738707 since: 2021-12-30T16:06:54Z

*Publisher:*

*Published*

DOI:10.1063/1.4890394

*Terms of use:*

openAccess

Anyone can freely access the full text of works made available as "Open Access". Works made available

*Publisher copyright*

(Article begins on next page)

# Non-contact direct measurement of the magnetocaloric effect in thin samples

F. Cugini<sup>1,a)</sup>, G. Porcari<sup>1</sup>, M. Solzi<sup>1</sup>

<sup>1</sup>*Department of Physics and Earth Sciences, University of Parma, Parco Area delle Scienze 7/A, 43124 Parma, Italy*

An experimental setup, based on a non-contact temperature sensor, is proposed to directly measure the magnetocaloric effect of samples few micrometers thick. The measurement of the adiabatic temperature change of foils and ribbons is fundamental to design innovative devices based on magnetocaloric thin materials or micro-structuring bulk samples. The reliability of the proposed setup is demonstrated by comparing the measurements performed on a bulk gadolinium sample with the results obtained by an experimental setup based on a Cernox bare chip thermoresistance and by in-field differential scanning calorimetry. We show that this technique can measure the adiabatic temperature variation on gadolinium sheets as thin as 27  $\mu\text{m}$ . Heat transfer simulations are added to describe the capability of the presented technique.

## I. INTRODUCTION

Solid-state magnetic refrigeration around room temperature is a promising technology for replacing the conventional gas compression/expansion technique. This technology not only permits to eliminate hazardous gases, which are at the basis of actual refrigerators, but it allows also an improvement of energy efficiency and the development of more compact and less noisy devices.<sup>1,2</sup> If we consider the growing demand of energy for refrigeration (for food conservation, comfort of living spaces and medical applications) and the concerns for ongoing environmental changes the great interest of research towards the development of this new technology is clear.<sup>3</sup>

At the basis of magnetic refrigeration is the magnetocaloric effect (MCE),<sup>4,5</sup> which is a variation of entropy ( $\Delta S_{iso}$ ) or of temperature ( $\Delta T_{ad}$ ) in a magnetic material due to the change of an applied magnetic field in isothermal or adiabatic conditions, respectively.<sup>6</sup> This effect is

maximum across magnetic phase transitions where the magnetization change, as a function of temperature or magnetic field, is larger. In the last decade there has been a sharp increase in the research of new materials, showing a giant MCE across first order magnetic transitions near room temperature,<sup>3</sup> and in the development of many magnetic refrigeration prototypes.<sup>7</sup> An indirect characterization of the MCE can be performed by calorimetry under magnetic field<sup>8,9</sup> or by magnetization measurements.<sup>10</sup> Both these techniques require numerical processing of experimental data which usually generates a significant uncertainty (even 20-30%)<sup>11,12</sup> on the final estimations of  $\Delta T_{ad}(T,H)$ . The MCE, considered as an adiabatic temperature variation, can be also directly measured during the variation of an applied magnetic field. Many experimental setups have been proposed, which are all based on the principle of measuring the sample temperature, in quasi-adiabatic conditions, while the field is turned on or off. This allows to reduce the experimental errors<sup>13</sup> and to observe directly the thermodynamic response of the material to the magnetic stimulus, the most valuable specific parameter concerning practical magnetocaloric applications.<sup>14,15</sup> The realization of nearly-ideal adiabatic conditions is the trickiest aspect of such techniques. Fast sweeps, obtained turning on or off an electromagnet<sup>13,16</sup> or by the application of pulsed fields<sup>16</sup> or otherwise by moving the sample inside a steady field,<sup>17,18</sup> can improve the adiabatic conditions during the measurement. Generally, the temperature measurements are performed with thermocouples<sup>16,18</sup> or high precision thermoresistances, little influenced by the magnetic field change.<sup>13,17</sup> Some experimental setups based on non-contact temperature measurement techniques, like thermoacoustic methods<sup>19, 20</sup> or thermography<sup>21</sup> have also been proposed. Both these techniques, thanks to the absence of contact between sample and sensor, can be suitable for the characterization of thin samples, although some drawbacks still limit their use. Thermoacoustic methods estimate the magnetic field induced temperature change by superimposing to a magnetic ac field a static or slowly sweeping dc field. The  $\Delta T$  values obtained by using these techniques are proved to be accurate, nevertheless they are far from probing the material's response in operating conditions (i.e. under fast sweeping fields). Thermocameras characterized by a good temperature resolution ( $dT_{min} < 0.1$  K) are appropriate for a spatially resolved study of the material's surface temperature, while often they are expensive and not handy to simulate thermomagnetic cycles, due to the presence of moving mechanical parts.

In the last years, for the development of real working refrigeration devices, it has been highlighted the importance of reporting further properties of materials (such as thermal and electric conductivity and mechanical hysteresis) and of studying their response in repeated

thermomagnetic cycles.<sup>13,22,23</sup> At the same time, the idea of designing micro-structures able to optimize the heat transfer<sup>1</sup> and of realizing solid state (micro-)miniaturized cooling devices<sup>14, 24</sup> boosted the need of studying the MCE in low-dimensional materials as thin sheets, ribbons and thin films. In recent literature many works can be found treating growth, structural and magnetic characterization of materials of such kind.<sup>25-31</sup> Some tries to directly measure the MCE in these systems have been explored,<sup>21,32-34</sup> however, till today this field is rather lacking, due to the intrinsic difficulties of this type of measurement. A handy instrument, which does not need of a complex post-measurement elaboration, has not yet been proposed. In this work we present a new experimental setup, based on a non-contact commercial temperature sensor, a thermopile, for the direct MCE measurement on very thin samples. This sensor is mechanically stable, cheap, it is characterized by a good sensitivity and a low noise. The small sensor response time and the absence of contact with the sample give the possibility of reducing the measurement time and of achieving good quasi-adiabatic conditions. These benefits permit the use of this sensor for characterizing thin samples and for studying the MCE in high frequency cycles. The capability of this technique is shown by measuring gadolinium samples down to 20  $\mu\text{m}$  thick. In the final part we present a guideline to figure out the time-scale required to measure thinner samples.

## II. EXPERIMENTAL SETUP

The structural part of the realized instrument is composed of a long plate of copper, water-cooled, which acts as a multipurpose optical bench, on which one can align the temperature sensor and the sample holder (see Fig. 1). The plate is inserted in a cylindrical vacuum chamber (diameter: 22 mm, maximum vacuum:  $10^{-5}$  mbar), placed in between the poles of a low-inductive electromagnet which is able to generate a magnetic field sweep up to 2.4 T. The time taken by the field source to reach the maximum field ( $H_{max}$ ) is about 1 s while the time constant of the exponential rise (63% of  $H_{max}$ ) is lower than 0.3 s. The temperature measurement is performed with a commercial thermopile sensor (ZTP-135SR of General Electric Company<sup>©</sup>) composed of a  $0.7 \times 0.7 \text{ mm}^2$  photo-absorbing membrane placed on the top of a serially-interconnected array of 60 thermoelectric junctions. The cold junctions are placed in contact with a heat sink at the base of the sensor. The thermopile is locked in a hermetically-sealed package, with a silicon window allowing the transmission of 6  $\mu\text{m}$  to 16

$\mu\text{m}$  radiation (thermal IR radiation). The output voltage reflects the difference between the sample temperature, placed in front of the sensor window, and the temperature of its base. The output signal is amplified and filtered with a notch filter ( $f_0=50$  Hz) and a low-band filter ( $f_c: 200$  Hz) then acquired through a DAQ (BNC-2120 of National Instruments) at a sampling frequency of 10 kHz. It was verified that the magnetic field does not perturb the thermopile response. A short spike of electric noise appears however during the field change. This noise, independent of the sensor signal, is subtracted from the measurements. The repeatability of the temperature measurement has been verified by iterating the observation of a copper plate whose temperature was changed and stabilized with a resistive heater and a Pt100 sensor. The time constant of the sensor ( $\tau=27$  ms) has been experimentally estimated by placing an optical chopper between the sensor window and a copper plate kept at a constant temperature (source of constant IR radiation). In this way the sensor receive an IR square-wave. The time constant is considered as the time needed for the sensor signal, at every half-period, to reach 63% of its maximum value (see Fig.2). It has to be noticed that the minimum time required for achieving the maximum signal value is about 85 ms and hence the operative frequency limit in case of simulation of thermomagnetic cycles should be about 6 Hz.

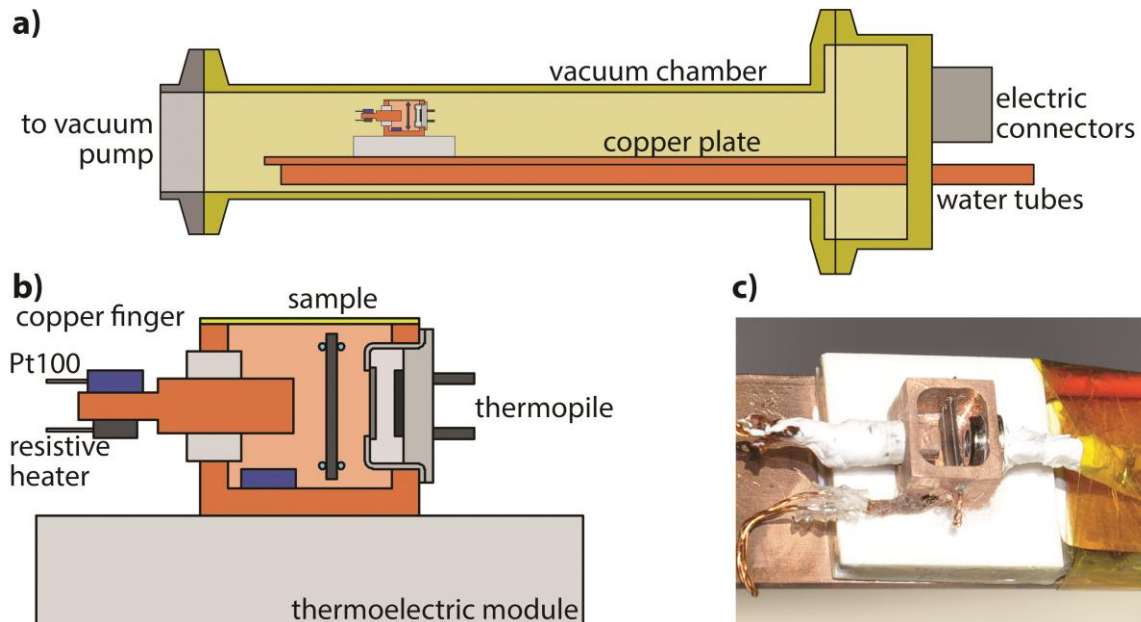


FIG. 1. Sketch of the experimental setup. (a) Vacuum chamber with the optical copper bench. (b) Copper box with sensor (on the right side), sample and copper finger (on the left side). (c) Top view of the sketch b).

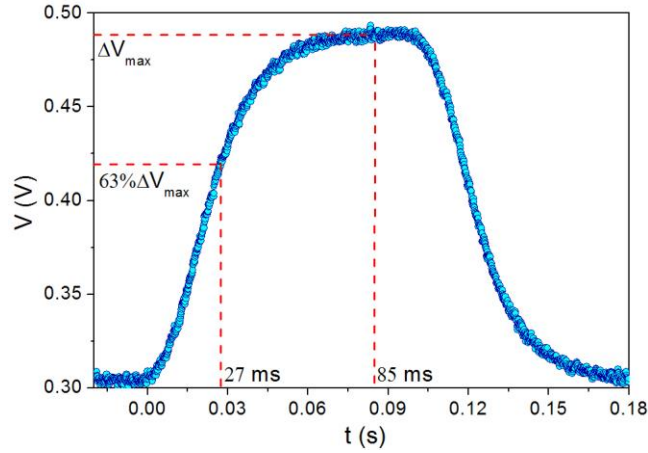


FIG. 2. Response curve of the thermopile exposed to a square wave, obtained chopping the IR radiation emitted from a copper plate kept at a constant temperature. The time constant of the sensor is the time needed for the signal to reach 63% of its maximum value.

The sensor and the sample are placed in a copper box ( $8 \times 9 \times 7 \text{ mm}^3$  – see Fig. 1), closed on the top with a brass plate thermally connected to the box by a thermoconductive paste (Arctic Silver® Ceramique,  $k = 7 \text{ W m}^{-1} \text{ K}^{-1}$ ). The sensor is inserted in a face of the box and thermally connected with it in order to keep both at the same temperature. The sample is suspended at the centre of the box with a frame of nylon wires. This solution permits to reduce the thermal contact between the sample and the environment and so to minimize the heat lost because of conductive dissipation. The sample is placed 1 mm away from the sensor so that a minimum surface of  $4.5 \times 4.5 \text{ mm}^2$  is enough to fully cover the view angle of the sensor. This helps to reduce the error due to background radiation. The longer axis of the sample is positioned parallel to the magnetic field to minimize the effects of shape anisotropy. A thermoelectric module, located under the box and in contact with the water-cooled plate, and a Pt100 sensor allow to control and stabilize the box temperature ( $T_b$ ) between 260 K and 350 K (see Fig. 1). The thermoconductive paste ensures a good thermal contact between the box and the module. The heat flux radiated by the sample, thus the voltage signal of the thermopile, is ruled by the surface emissivity, which is peculiar of every measured specimen. A solution to overcome this drawback could be to cover the surface with a thin layer of black paint in order to maximize and standardize the emissivity for every sample to be measured. This allows using the same calibration when measuring different materials.<sup>21,35</sup> In this way however we measure the temperature change of the black paint. As suggested in ref. [36] and [37] the calibration may be repeated for each sample, not painted, in order to observe the direct effect of the sample surface. In our case the calibrations are performed, for each sample, placing in

contact with the back side of the sample, by a thermoconductive paste, a thermally controlled copper finger (thermal bath) with a Pt100 sensor and a resistive heater. An ITC503 temperature controller (Oxford Instruments) is used to stabilize the temperature of the finger, independently of  $T_b$  (which is kept constant), within 0.01 K. The calibrations are obtained sweeping the temperature (heating and cooling) with a rate lower than  $0.5 \text{ Kmin}^{-1}$  to minimize the thermal gradient between copper finger and sample. The short temperature range (about 5 K above  $T_b$ ) of every calibration makes possible to fit the obtained  $V(T)$  curve with a linear function  $T(V)=aV+b$ . Small variations of the coefficients have been observed on repeating the calibration. This contributes with an error of 0.1 K to the measured temperature. To reduce the error due to background IR radiation we repeated the calibration at every  $T_b$ . During the measurement of the adiabatic temperature variation, the copper finger is removed from the box and the sample remains thermally insulated from the environment.

### III. EXPERIMENTAL RESULTS

The instrument reliability has been tested by measuring the  $\Delta T_{ad}(T)$  of a gadolinium bulk sample (Goodfellow 99.9% pure, dimensions:  $5 \times 3 \times 2 \text{ mm}^3$ , mass: 252 mg) induced by an internal magnetic field change  $\mu_0 \Delta H = 1.75 \pm 0.1 \text{ T}$ . This value was estimated considering a demagnetizing factor of 0.2 and an external magnetic field of  $1.9 \pm 0.1 \text{ T}$ . Figure 3 shows the good agreement between the measured  $\Delta T_{ad}(T)$  values and those obtained on the same sample by a previously described setup for direct measurement<sup>13</sup>, based on a Cernox bare-chip temperature sensor, and by in-field differential scanning calorimetry (DSC).<sup>13</sup> It can be also appreciated from figure 3 that the direct techniques show smaller error-bars when compared to those obtained from calorimetry<sup>12,13</sup>, which have been calculated following the standard method described in Ref. [11]. In particular the error bars of  $\Delta T_{ad}$  deduced from the in-field DSC measurement (dashed lines in Fig. 3) result from error propagation in the integration of specific heat<sup>12</sup>. This confirms the suitability of the direct techniques for estimating the magnetocaloric effect.

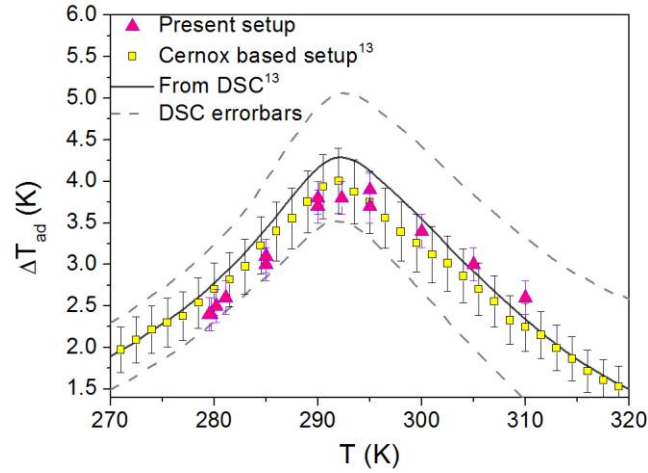


FIG. 3.  $\Delta T_{ad}(T)$ , in a  $\mu_0\Delta H=1.75\pm 0.1$  T, for a bulk sample of gadolinium obtained from: present setup (triangles), probe based on a Cernox temperature sensor presented in Ref. [13] (squares) and in-field DSC (line) also described in Ref. [13]. The dashed lines represent the error-bars on  $\Delta T_{ad}$  deduced from elaboration of DSC measurement.

The adiabatic temperature variation of a gadolinium sheet with decreasing thickness (down to 13  $\mu\text{m}$ ) has been measured to probe the capability of this experimental setup. We preferred to smooth progressively the same starting sheet (Goodfellow, 99.9% purity, thickness: 100  $\mu\text{m}$ , surface:  $5.7\times 7.0$   $\text{mm}^2$ ) to rule out the effect of unknown impurities content when comparing the  $\Delta T_{ad}$  of samples with different thicknesses. Figure 4 shows a single measurement of  $\Delta T_{ad}$  at 292 K of a sample  $58\pm 2$   $\mu\text{m}$  thick (mass:  $18.0\pm 0.1$  mg) for a magnetic field change  $\mu_0\Delta H=2.0\pm 0.05$  T. The magnetic field profile, measured with a Lakeshore 460 3-channel Hall-effect gaussmeter, is superimposed to the measurement. It can be appreciated that the sensor does not introduce a relevant delay in the measurement since its response time is faster than the magnetic field rise-time. The  $\Delta T_{ad}$  obtained ( $3.9\pm 0.2$  K) is in agreement with other data reported in literature,<sup>20,38</sup> considering the strong dependence of the effect from the presence of impurities and Gd oxide,<sup>39</sup> emphasized in this case by the large surface-to-volume ratio.

The measured  $\Delta T_{ad}$  of the same sheet with five different thicknesses ( $80\pm 2$   $\mu\text{m}$ ,  $58\pm 2$   $\mu\text{m}$ ,  $37\pm 2$   $\mu\text{m}$ ,  $27\pm 2$   $\mu\text{m}$ ,  $13\pm 2$   $\mu\text{m}$ ) for  $\mu_0\Delta H = 1.00\pm 0.05$  T and  $2.00\pm 0.05$  T is reported in figure 5. All the measurements have been performed at  $292.0\pm 0.2$  K. It can be observed that the measured values ( $3.8\pm 0.2$  K,  $2.2\pm 0.2$  K) are constant within the experimental error down to 27  $\mu\text{m}$ . The thinner sample (13  $\mu\text{m}$ ) shows a decrease of the measured effect due to the heat lost during the field sweep (field rise time  $t\sim 1$  s).



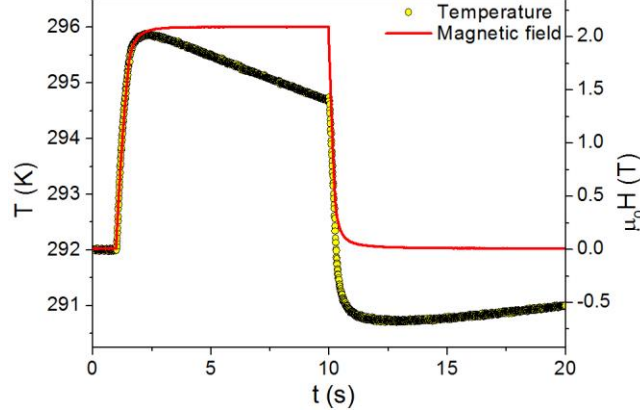


FIG. 4. Direct  $\Delta T_{ad}$  measurement of a gadolinium sheet (58  $\mu\text{m}$  thick) in  $\mu_0\Delta H=2.0$  T both switching the field on and off. The magnetic field profile (red line) is superimposed to the temperature profile of the sample (yellow points).

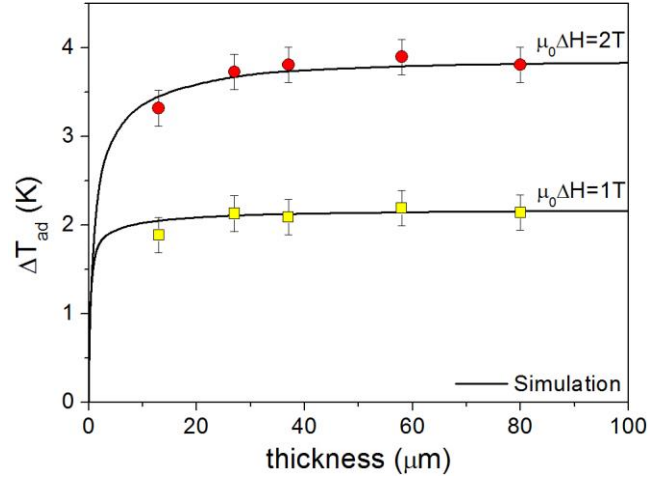


FIG. 5.  $\Delta T_{ad}$  of a gadolinium sheet as a function of its progressively reduced thickness for  $\mu_0\Delta H = 1.0$  T (yellow squares) and 2.0 T (red circles). The result of a numerical simulation of the thermodynamic system (black line) is superimposed to the experimental data.

We have performed, then, heat transfer simulations to better explain the experimental results and to make a prediction about the possibility of measuring thinner samples. We have considered that the thermal conductance within the material is much higher than the one between sample and environment. This fact has allowed us to assume a spatially uniform temperature inside the sheet. Two contributions to the heat exchange have been taken into account: the MCE as a heat source developing inside the sheet for a time interval equal to the rise time of the external field and the heat dissipated through radiation. The first quantity has been calculated by using the isothermal entropy change ( $\Delta S_{iso}$ ) obtained from magnetic measurements:  $Q_{MCE} = \Delta S_{iso} m T$ , where  $m$  is the sample mass. Its time rate (equation 1) has

been obtained considering that the temperature variation is proportional to the applied field as reported in ref. [40].

$$W_{MCE}(t) = Q_{MCE} \frac{1}{H_{max}^{2/3}} \frac{dH(t)^{2/3}}{dt} \quad (1)$$

The second contribution is the heat radiated from the sample surface:

$$W_{irr}(t) = \varepsilon \sigma S (T(t)^4 - T_b^4) \quad (2)$$

where  $S$  is the sample surface,  $\varepsilon=0.3$  its emissivity,  $c_p = 315 \text{ Jkg}^{-1}\text{K}^{-1}$  its specific heat,  $T_b$  the box temperature and  $\sigma$  the Boltzmann constant. The temperature profile of the sample as a function of time has been calculated using equation (3).

$$T(i+1) - T(i) = \frac{(W_{MCE} - W_{irr})\Delta t}{c_p m} \quad (3)$$

The emissivity  $\varepsilon$  of gadolinium has been obtained through a best-fit, based on Eq. (3), of the decreasing part of the measured  $T(t)$ , corresponding to the thermal relaxation after the peak value (see Fig. 6).

The result for a  $27 \mu\text{m}$  thick gadolinium sheet (mass= $8.4 \pm 0.1 \text{ mg}$ ) and a magnetic field change  $\mu_0 \Delta H = 1 \text{ T}$  is shown in figure 6. The simulation follows the experimental data during the whole period of the experiment. This outcome highlights that the quasi-adiabatic conditions achieved with this setup are good enough to consider radiation as the main source of heat losses.

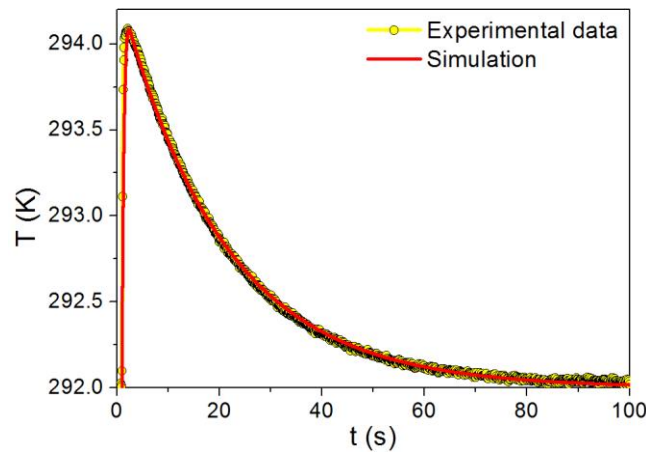


FIG. 6. Experimental (yellow points) and simulated (red line) temperature profiles of a gadolinium sheet (thickness: 27 $\mu$ m) during and after the magnetic field ramp ( $\mu_0\Delta H=1.0$  T).

The simulation has been repeated changing the thickness of the sheets to obtain estimation of the maximum expected  $\Delta T_{ad}$ . This calculation, reported in figure 5 (black lines), confirms that just below a thickness of 20  $\mu$ m the radiation heat losses avoid a correct estimation of the sample temperature change. To measure even thinner samples it is necessary to reduce the rise time of the magnetic field sweep together with the total measurement time-scale. The simulation presented above can be used to predict the fraction of detectable  $\Delta T_{ad}$  as a function of the measurement time-scale. Keeping fixed the sheet surface ( $S=5.6\times 7.0$  mm<sup>2</sup>), the simulation has been repeated, for every thickness, decreasing the time constant ( $\tau$ ) of the exponential field sweep:  $H(t) = H_{Max}(1 - e^{-\frac{t}{\tau}})$ . The sensor response time has been considered negligible compared to  $\tau$ . Figure 7 shows the fraction of  $\Delta T_{ad}$ , which may be picked up in samples of gadolinium with thickness between 1 mm and 10 nm and with magnetic field time constants ranging from 10<sup>2</sup> s to 10<sup>-4</sup> s. The black points represent the maximum time scale required to measure at least 95% of the  $\Delta T_{ad}$  for a given thickness. This threshold is imposed by a relative experimental error of about 5%. The area under this curve shows the combination of field time constant and sample thickness that allows the almost full measurement of  $\Delta T_{ad}$ . The five cyan points drawn in figure 7 represent the experimental measurements on the five thicknesses of the gadolinium sheet. As experimentally verified, four of these are enough to measure, within the experimental errors, about 95% of the  $\Delta T_{ad}$ . The thinnest sample, instead, falls significantly above the curve. In this case we report  $\Delta T_{ad} = 3.3\pm 0.2$  K, equal to 87% ( $\pm 5\%$ ) of  $\Delta T_{ad}$  measured in the thicker sample, for which the heat dissipation during the field sweep is negligible. Inset of figure 7 has been added to underline the proportionality between the time constant required to measure at least 95% of  $\Delta T_{ad}$  and the sample volume-to-surface ratio ( $V/S$ ). This outcome can be obtained by integration of equation (3). The MCE is approximated as linearly dependent to the external magnetic field while the heat emitted through radiation is considered proportional to the temperature difference between sample and environment.

$$t_{95\%} = (1 - 95\%) \frac{2c_p\rho V}{\varepsilon\sigma T_b^3 S} \quad (4)$$

This relation pinpoints that, for samples with larger heat capacity and lower transition temperature, the full  $\Delta T_{ad}$  can be measured with longer time constants of the field change. On the other hand, in samples characterized by larger surface, higher emissivity and higher transition temperature, radiation losses will be more pronounced, thus requiring faster field sweeps. In the case of first order transitions, which may be as well measured with this setup, the presence of latent heat would increase the ratio between the heat generated inside the sample and that dissipated from it, improving the quasi-adiabatic conditions and allowing the measurement of even thinner samples. This analysis, reproducible for other sample dimensions, materials and field sweeps, helps to figure out useful clues to design new experimental setups able to measure thinner systems.

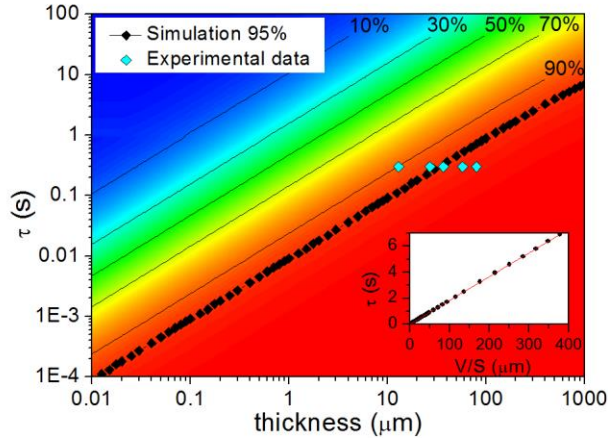


FIG. 7. Simulation of the detectable fraction of  $\Delta T_{ad}$  as a function of the sample thickness and time constant of the field change in case of gadolinium sheets. The black points mark 95% of  $\Delta T_{ad}$ , while the cyan points are the experimental results also reported in figure 5. Inset: linear dependence of the time constant of the field sweep as a function of the volume to surface ratio.

#### IV. CONCLUSION

In this work we present a new experimental setup, based on a commercial thermopile sensor able to directly measure the magnetocaloric effect of bulk and thin sheet samples. This non-contact technique allows to reproduce good quasi-adiabatic conditions needed to pick up the absolute  $\Delta T_{ad}$  in gadolinium sheets as thin as 27  $\mu\text{m}$  without the need of a complex post-measurement elaboration. Simulations of the measurement system confirmed the experimental results and predict the time-scale of the magnetic field change required for measuring thinner samples. These calculations moreover show that in case of first order materials even thinner samples could be successfully measured thanks to the contribution of latent heat.

We believe that this technique is an ideal solution both to directly measure the MCE of samples with reduced thickness and to reproduce high frequency (up to 6 Hz, as deduced from the total response time of the sensor) thermomagnetic cycles for testing the material response in operating conditions. The use of thermopiles moreover can be extended to measure directly other caloric effects in thin samples. The proposed non-contact technique, when studying Electrocaloric, Barocaloric and Elastocaloric effects,<sup>41</sup> may become an undeniable solution to isolate the temperature sensor from electric or mechanic stresses thus improving the measurement quality and the lifetime of the technique.

### Acknowledgements

Thanks are due to Dr. Davide Delmonte of the Department of Physics and Earth Sciences (University of Parma) for his willingness in preparing the gadolinium sheets and to Dr. Chiara Pernechele of the Department of Physics and Earth Sciences (University of Parma) for helpful discussions.

### References

- <sup>1</sup> A. Kitanovski, and P. W. Egolf, *Int. J. Refrig.* **33**, 449 (2010).
- <sup>2</sup> K. A. Gschneidner, and V. K. Pecharsky, *Int. J. Refrig.* **31**, 945 (2008).
- <sup>3</sup> O. Gutfleisch, M. A. Willard, E. Brück, C. H. Chen, S. G. Sankar, and J. P. Liu, *Adv. Mat.* **23**, 821 (2011).
- <sup>4</sup> A. M. Tishin, and Y. I. Spichkin, *The Magnetocaloric Effect and its Applications* (IOP, 2003).
- <sup>5</sup> A. Smith, C. R. H. Bahl, R. Bjørk, K. Englebrecht, K. K. Nielsen, and N. Pryds, *Adv. Energy Mater.* **2**, 1288 (2012).
- <sup>6</sup> E. Brück, *Magnetocaloric refrigeration at ambient temperature*, in *Handbook of Magnetic Materials* edit by K. H. J. Buschow (Elsevier, Amsterdam, 2007), Vol. 17, Chap. 4.
- <sup>7</sup> B. Yu, M. Liu, P. W. Egolf, and A. Kitanovski, *Int. J. Refrig.* **33**, 1029 (2010).
- <sup>8</sup> V. Basso, C. P. Sasso, and M. Küpferling, *Rev. Sci. Instrum.* **81**, 113904 (2010).
- <sup>9</sup> Y. Miyoshi, K. Morrison, J. D. Moore, A. D. Caplin, and L. F. Cohen, *Rev. Sci. Instrum.* **79**, 074901 (2008).
- <sup>10</sup> L. Caron, Z. Q. Ou, T. T. Nguyen, D. T. Cam Thanh, O. Tegus, and E. Brück, *J. Magn. Magn. Mater.* **321**, 3559 (2009).
- <sup>11</sup> V. K. Pecharsky, and K. A. Gschneidner, *J. Appl. Phys.* **86**, 565 (1999).
- <sup>12</sup> G. Porcari, F. Cugini, S. Fabbrici, C. Pernechele, F. Albertini, M. Buzzi, M. Mangia, and M. Solzi, *Phys. Rev. B* **86**, 104432 (2012).
- <sup>13</sup> G. Porcari, M. Buzzi, F. Cugini, R. Pellicelli, C. Pernechele, L. Caron, and M. Solzi, *Rev. Sci. Instrum.* **84**, 073907 (2013).
- <sup>14</sup> S. Fähler, U. K. Rößler, O. Kastner, J. Eckert, G. Eggeler, H. Emmerich, P. Entel, S. Müller, E. Quandt, and K. Albe, *Adv. Energy Mater.* **14**, 10 (2012).
- <sup>15</sup> B. Schwarz, N. Mattern, J. D. Moore, K. P. Skokov, O. Gutfleisch, and J. Eckert, *J. Magn. Magn. Mater.* **323**, 1782 (2011).

- <sup>16</sup> S. Yu. Dan'kov, A. M. Tishin, V. K. Pecharsky, and K. A. Gschneidner, *Rev. Sci. Instrum.* **68**, 2432 (1997).
- <sup>17</sup> B. R. Gopal, R. Chahine, and T. K. Bose, *Rev. Sci. Instrum.* **68**, 1818 (1997).
- <sup>18</sup> J. Kamarad, J. Kastil, and Z. Arnold, *Rev. Sci. Instrum.* **83**, 083902 (2012).
- <sup>19</sup> B. R. Gopal, R. Chahine, M. Földeàki, and T. K. Bose, *Rev. Sci. Instrum.* **66**, 232 (1995).
- <sup>20</sup> A. O. Guimarães, M. E. Soffner, A. M. Mansanares, A. A. Coelho, A. Magnus, G. Carvalho, M. J. M. Pires, S. Gama, and E. C. da Silva, *Phys. Rev. B* **80**, 134406 (2009).
- <sup>21</sup> D. V. Christensen, R. Bjørk, K. K. Nielsen, C. R. H. Bahl, A. Smith, and S. Clausen, *J. Appl. Phys.* **108**, 063913 (2010).
- <sup>22</sup> K. G. Sandeman, *Script. Mater.* **67**, 566 (2012).
- <sup>23</sup> J. Lyubina, *J. Appl. Phys.* **109**, 07A902 (2011).
- <sup>24</sup> D. J. Silva, B. D. Bordalo, A. M. Pereira, J. Ventura, and J. P. Araùjo, *Appl. Energy* **93**, 570 (2012).
- <sup>25</sup> O. Gutfleisch, A. Yan, and K. H. Müller, *J. Appl. Phys.* **97**, 10M305 (2005).
- <sup>26</sup> Z. B. Li, Y. D. Zhang, C. F. Sánchez-Valdés, J. L. Sánchez Llamazares, C. Esling, X. Zhao, and L. Zuo, *Appl. Phys. Lett.* **104**, 044101 (2014).
- <sup>27</sup> Z. Q. Ou, L. Zhang, H. H. Dung, L. van Eijck, A. M. Mulderes, M. Avdeev, N. H. van Dijk, and E. Brück, *J. Magn. Magn. Mater.* **340**, 80 (2013).
- <sup>28</sup> N. T. Trung, J. C. P. Klaasse, O. Tegus, D. T. Cam Thanh, K. H. J. Buschow, and E. Brück, *J. Phys. D* **43**, 015002 (2010).
- <sup>29</sup> R. L. Hadimani, I. C. Nlebedim, Y. Melikhov, and D. C. Jiles, *J. Appl. Phys.* **113**, 17A935 (2013).
- <sup>30</sup> X. Moya, L. E. Hueso, F. Maccherozzi, A. I. Tovstolytkin, D. I. Podyalovskii, C. Ducati, L. C. Phillips, M. Ghidini, O. Hovorka, A. Berger, M. E. Vickers, E. Defay, S. S. Dhesi, and N. D. Mathur, *Nat. Mater.* **12**, 52 (2012).
- <sup>31</sup> M. Solzi, C. Pernechele, M. Ghidini, M. Natali, and M. Bolzan, *J. Magn. Magn. Mater.* **322**, 1565 (2010).
- <sup>32</sup> J. Y. Law, V. Franco and R. V. Ramanujan, *J. Appl. Phys.* **110**, 023907 (2011).
- <sup>33</sup> A. M. Mansanares, F. C. G. Gandra, M. E. Soffner, A. O. Guimarães, E. C. da Silva, H. Vargas, and E. Marin, *J. Appl. Phys.* **114**, 163905 (2013).
- <sup>34</sup> A. M. Aliev, A. B. Batdalov, I. K. Kamilov, V. V. Koledov, V. G. Shavrov, V. D. Buchelnikov, J. Garcia, V. M. Prida, and B. Hernando, *Appl. Phys. Lett.* **97**, 212505 (2010).
- <sup>35</sup> S. C. Santos, Master thesis, Universidade de Aveiro, Aveiro, 2010.
- <sup>36</sup> G. Sebald, L. Seveyrat, J. F. Capsal, P. J. Cottinet, and D. Guyomar, *Appl. Phys. Lett.* **101**, 022907 (2012).
- <sup>37</sup> S. Kar-Narayan, S. Crossley, X. Moya, V. Kovacova, J. Abergel, A. Bontempi, N. Baier, E. Defay, and N. D. Mathur, *Appl. Phys. Lett.* **102**, 032903 (2013).
- <sup>38</sup> S. Yu. Dan'kov, A. M. Tishin, V. K. Pecharsky and K. A. Gschneidner, *Phys. Rev. B* **57**, 3478 (1998).
- <sup>39</sup> F. Canepa, S. Cirafici, M. Napoletano, M. R. Cimberle, L. Tagliafico, and F. Scarpa, *J. Phys. D: Appl. Phys.* **41**, 155004 (2008).
- <sup>40</sup> M. D. Kuz'min, K. P. Skokov, D. Yu. Karpenkov, J. D. Moore, M. Richter, and O. Gutfleisch, *Appl. Phys. Lett.* **99**, 012501 (2011).
- <sup>41</sup> X. Moya, S. Kar-Narayan, and N. D. Mathur, *Nature Mater.* **13**, 439 (2014).